Gordon Kent (S'47–A'52–M'56–SM'73) was educated at the University of Wisconsin, Madison (B.S.E.E.) and Stanford University (M.S.E.E. and Ph.D., 1953). While at Stanford he worked as a Research Assistant in the Microwave Laboratory where much of the development of the Stanford Linear Accelerator was taking place, and he was awarded a Sperry Fellowship.

Following graduation he was employed as a Research Engineer by the Institute for Advanced Studies at Princeton, NJ to work on the development of the Institute's pioneer computer. Part of the group headed by the late John von Neumann, he was designated as one of the "computer pioneers" by the American Federation of Information Processing Societies and the 1975 National Conference Steering Committee. From 1954 to 1957 he was a Research Fellow in Electronics at Harvard University. Much of his research during that period concerned a microwave oscillator that later came to be known as the "Osaka tube". In 1957 he joined the Electrical Engineering faculty at Syracuse University, Syracuse, NY, where he presently holds the rank of Professor.

The diverse fields in which Dr. Kent has published include numerical analysis, engineering education, solar cells, electron beams, microwave properties of plasmas, and nonlinear waves.

He is a member of the American Physical Society, Division of Plasma Physics, and the Plasma Science Society.

Donald D. Weiner (S'54–M'60) was born in Boston, MA, on October 30, 1934. He received the S.B., S.M., and E.E. degrees from M.I.T., Cambridge, MA in 1956, 1958, and 1960, respectively, and the Ph.D. degree from Purdue University, Lafayette, IN in 1964, all in electrical engineering.

He has worked for the Philco Corporation, Philadelphia, PA, General Electronic Laboratories, Boston, MA, and Sylvania Applied Research Laboratory, Waltham, MA. He has taught at M.I.T., the University of Miami, and Purdue University. He joined Syracuse University in 1964 as Assistant Professor in the Department of Electrical and Computer Engineering where he was promoted to Associate Professor and Professor in 1968 and 1973, respectively. His current research interests are in the analysis, modeling, and identification of weakly nonlinear systems and in the effects of interference on analog and digital equipments.

Dr. Weiner is a co-author with John Spina of the Van Nostrand Reinhold book "Sinusoidal Analysis and Modeling of Weakly Nonlinear Circuits: With Application to Nonlinear Interference Effects."

A Study of the Noise-Temperature Performance of a Satellite Communications Low-Noise Amplifier Subsystem

MITSUGI KAJIKAWA

Abstract—**The heart of the low-noise amplifier (LNA) subsystem is the parametric amplifier which consists of a parametric amplifier proper and a circulator. The LNA subsystem can be simplified into an equivalent circuit, to evaluate its noise-temperature performance by assuming that it consists of a parametric amplifier proper and a circulator, which in its overall sense includes the additional components of the input line as elements in one arm of the circulator. Using this simplified equivalent circuit, the noise-temperature performance is analyzed theoretically and provides a precise value for the LNA subsystem noise-temperature degradation, the noise-temperature increase of the earth-station receiving system caused by connecting an actual antenna to the subsystem and the measurement error of the HOT/COLD load noise temperature measurement method.**

Manuscript received October 22, 1981; revised February 9, 1982.

The author is with the Microwave and Satellite Communications Division of Nippon Electric Company, Ltd., Ikebe-cho, Midori-ku, Yokohama, Japan.

I. INTRODUCTION

IN A SATELLITE communications earth station, the low-noise amplifier (LNA) subsystem is one of the most important subsystems and its noise temperature performance makes a major contribution to the figure of merit

0018-9480/82/0700-1068$00.75 ©1982 IEEE

G/T of the earth-station receiving system. The LNA subsystem is usually in a redundant configuration with two identical LNA units connected to a protection switch. In addition, several components such as a transmit reject filter and directional coupler are connected to the input port of the LNA subsystem. Currently, the heart of the LNA unit is a parametric amplifier which is followed by a low-noise FET amplifier. Consequently, the noise-temperature performance of the LNA subsystem is influenced by the parametric amplifier, redundancy protection switch, transmit reject filter, directional coupler, and FET amplifier.

Though the noise-temperature performance of a parametric amplifier has been discussed in several papers [1], [2], that of the overall LNA subsystem has not been dealt with in any paper. Moreover, those papers analyzing the parametric amplifier assume the circulator, which is a key element of a parametric amplifier, is an ideal circulator and thus are not truly valid for an actual application. One paper treats effects of mismatch in parametric amplifier system noise measurements [3]. However, its analysis does not reach the effect caused by the circulator's mismatch.

In actual fact, a noise-temperature degradation of even 1 K cannot be neglected, and therefore an analysis of the overall noise-temperature performance is much more important.

In order to satisfy this requirement, this paper describes in detail the theoretical analysis of the LNA subsystem noise-temperature performance. The starting point of this theoretical analysis is not to treat the circulator as an ideal circulator and include in its overall equivalent circulator those components which are connected to the input port of the parametric amplifier. Consequently, the development of this theory is to analyze the effect, given by the circulator in its overall sense, on the noise-temperature performance of a reflection-type amplifier. The noise-temperature contribution from the following FET amplifier is not included in this discussion, because it can be easily estimated by dividing the noise temperature by the gain of the parametric amplifier.

The effect of the circulator on the overall noise-temperature performance can be classified into three categories: 1) the noise temperature degradation of the LNA subsystem itself; 2) when the LNA subsystem is connected to an actual antenna, the noise temperature of the earth-station receiving system increases due to the residual reflection coefficient of the antenna; and 3) the noise-temperature measurement error introduced by the HOT/COLD load-measurement method, due to the same residual reflection coefficients of these loads.

II. Equivalent Circuit

The equivalent circuit of the LNA subsystem is shown in Fig. 1. Therefore, it is clear that the noise temperature is influenced not only by the parametric amplifier proper but also by the circulator, the waveguide switch, the directional coupler, the transmit reject filter, and the following amplifier. Since the noise-temperature contribution, caused by the following amplifier, can be easily calculated by dividing the noise of the amplifier by the gain from the input to the output of the parametric amplifier, it is not discussed in this paper.

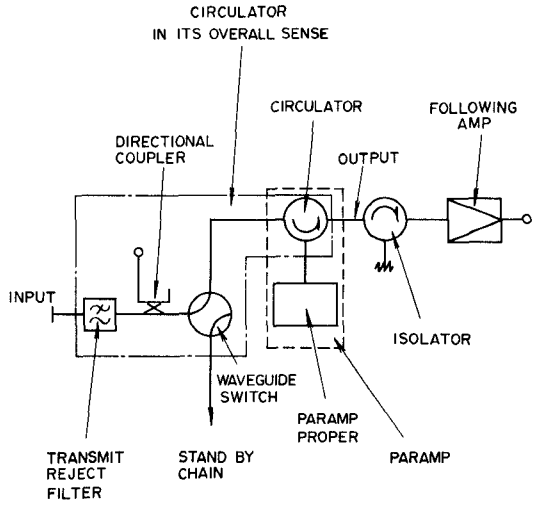

Fig. 1. Equivalent circuit of an LNA subsystem.

Those components connected in the input line to the circulator can be combined into a single two-port network and characterized by the scattering matrix

$$\begin{bmatrix} \gamma_{11} & \beta_{12} \\ \beta_{21} & \gamma_{22} \end{bmatrix}. \tag{1}$$

The circulator which is a seemingly symmetrical three-port one can also be characterized by the scattering matrix

$$\begin{bmatrix} \gamma_{10} & \beta_{10} & \alpha_{30} \\ \alpha_{10} & \gamma_{20} & \beta_{20} \\ \beta_{30} & \alpha_{20} & \gamma_{30} \end{bmatrix}. \tag{2}$$

In order to make the following analysis easy, the circulator in its overall sense defined as including those components connected in the input line as a part of its input port is introduced and characterized by the scattering matrix

$$\begin{bmatrix} \gamma_1 & \beta_1 & \alpha_3 \\ \alpha_1 & \gamma_2 & \beta_2 \\ \beta_3 & \alpha_2 & \gamma_3 \end{bmatrix} \tag{3}$$

which is a resultant of cascading (2) with (1) as shown in Appendix I.

Thus, the equivalent circuit can be converted into Fig. 2 showing a reflection-type amplifier proper connected to a circulator in its overall sense which is incomplete and not ideal.

The relation between the incident and reflection waves is expressed by

$$\begin{bmatrix} b_1 \\ b_2 \\ b_3 \end{bmatrix} = \begin{bmatrix} \gamma_1 & \beta_1 & \alpha_3 \\ \alpha_1 & \gamma_2 & \beta_2 \\ \beta_3 & \alpha_2 & \gamma_3 \end{bmatrix} \begin{bmatrix} a_1 \\ a_2 \\ a_3 \end{bmatrix}. \tag{4}$$

Now, the actual numbers of (3) are estimated to calculate the examples of the noise temperature in the following

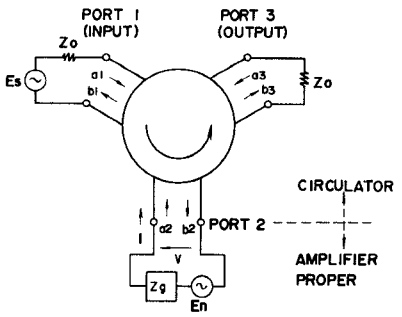

a1 : INCIDENT WAVE AT PORT i (i=1,2,3)
bi : REFLECTION WAVE AT PORT i (i=1,2,3)
Zo : CHARACTERISTIC IMPEDANCE PORT 1
Zg : IMPEDANCE OF AMPLIFIER PROPER
Es : VOLTAGE OF SIGNAL SOURCE
En : VOLTAGE OF NOISE SOURCE
V : VOLTAGE OF PORT 2
I : CURRENT OF PORT 2

Fig. 2. Equivalent circuit of an amplifier proper and a circulator.

description. As an example, assuming that the basic circulator's performance in the satellite communication band 3.7 to 4.2 GHz distributes in the range as follows:

$$\left.\begin{array}{ll} 10\log|\alpha_{i0}|^2, & -0.07\sim -0.15 \\ 10\log|\beta_{i0}|^2,\ 10\log|\gamma_{i0}|^2, & \text{less than } -23 \end{array}\right\} \quad (5)$$

and the two-port network in the same frequency band is characterized by

$$\left.\begin{array}{ll} 10\log|\beta_{12}|^2,\ 10\log|\beta_{21}|^2, & -0.07\sim -0.20 \\ 10\log|\gamma_{11}|^2,\ 10\log|\gamma_{22}|^2, & \text{less than } -27 \end{array}\right\}. \quad (6)$$

(3) is approximately calculated as follows:

$$\left.\begin{array}{ll} 10\log|\alpha_1|^2,\ 10\log|\alpha_3|^2, & -0.14\sim -0.35 \\ 10\log|\alpha_2|^2, & -0.07\sim 0.15 \\ 10\log|\beta_1|^2,\ 10\log|\beta_3|^2, & \text{less than } -23.07 \\ 10\log|\beta_2|^2, & \text{less than } -18.81 \\ 10\log|\gamma_1|^2, & \text{less than } -18.84 \\ 10\log|\gamma_2|^2,\ 10\log|\gamma_3|^2, & \text{less than } -22.62 \end{array}\right\}. \quad (7)$$

Thus, the following figures are used as the basis for presenting examples:

$$\left.\begin{array}{l} 10\log|\alpha_1|^2=-0.14,\ 10\log|\beta_1|^2=-23,\ 10\log|\gamma_1|^2=-19 \\ 10\log|\alpha_2|^2=-0.07,\ 10\log|\beta_2|^2=-19,\ 10\log|\gamma_2|^2=-23 \\ 10\log|\alpha_3|^2=-0.14,\ 10\log|\beta_3|^2=-23,\ 10\log|\gamma_3|^2=-23 \end{array}\right\}. \quad (8)$$

However, care should be taken of the fact that since those numbers are extreme ones they could cause rather alarming noise-temperature degradations in the following examples and if β_{i0} and γ_{i0} were improved the degradations would be significantly reduced.

III. Noise-Temperature Degradation of the LNA

Firstly, the noise-temperature degradation of the parametric amplifier proper caused by the circulator's incompleteness is analyzed, and then the noise caused by the absorption loss of the circulator itself is considered.

Finally, the noise generated by the isolator which also causes a noise-temperature increase is considered.

The total noise-temperature degradation can be estimated by summing up these three causes of noise-temperature degradation.

A. Noise Temperature Degradation of the Parametric Amplifier Proper

The reflection coefficient of the parametric amplifier proper is expressed as

$$\Gamma_a=\frac{Z_g-Z_0}{Z_g+Z_0}=\frac{a_2}{b_2}. \quad (9)$$

The gain from port 1 to port 3 is, by assuming $a_3=0$, $E_s\neq 0$, and $E_n=0$

$$|\Gamma_0|^2=\left|\frac{b_3}{a_1}\right|^2=\left|\frac{\alpha_1\alpha_2\Gamma_a}{1-\gamma_2\Gamma_a}+\beta_3\right|^2. \quad (10)$$

The voltage V and the current I at port 2 are expressed as

$$\left.\begin{array}{l} V=\sqrt{Z_0}\,(a_2+b_2) \\ I=\dfrac{1}{\sqrt{Z_0}}(a_2-b_2) \end{array}\right\}. \quad (11)$$

Since the following relations

$$\left.\begin{array}{l} \sqrt{Z_0}\,(a_2+b_2)=E_n-Z_g\left\{\dfrac{1}{\sqrt{Z_0}}(a_2-b_2)\right\} \\ b_2=\gamma_2 a_2 \end{array}\right\} \quad (12)$$

can be established by assuming $a_1=0$, $E_s=0$, and $E_n\neq 0$, it is possible, by using those relations, to obtain the expression for the noise power appearing at port 3. By applying several equation transformations as shown in Appendix II, the noise power of port 3 is expressed as

$$|\alpha_2 a_2|^2=|\alpha_2|^2\frac{|E_n|^2}{4R}\cdot\frac{(|\Gamma_a|^2-1)}{|1-\gamma_2\Gamma_a|^2} \quad (13)$$

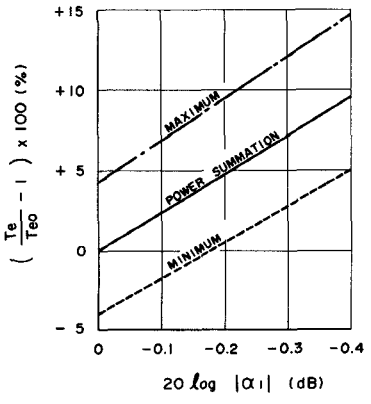

Fig. 3. Circulator's effect to T_e.

which is rewritten, by converting it into the equivalent value at port 1, using the basic noise-temperature expression,

$$T_e=\frac{|\alpha_2 a_2|^2}{KB|\Gamma_0|^2}=\frac{|E_n|^2}{4kRB}\left(1-\frac{1}{|\Gamma_a|^2}\right)\frac{1}{|\alpha_1|^2\left|1+\beta_3\dfrac{1-\gamma_2\Gamma_a}{\alpha_1\alpha_2\Gamma_a}\right|^2} \tag{14}$$

where k is the Boltzmann constant, and B is the bandwidth.

If an ideal circulator ($|\alpha_i|=1, \beta_i=0, \gamma_i=0$) is applied, (14) is expressed as

$$T_{e0}=\left(1-\frac{1}{|\Gamma_a|^2}\right)\left\{\frac{\text{exchangeable noise power [4]}}{kB}\right\}. \tag{15}$$

Accordingly, the noise-temperature degradation of the parametric amplifier can be calculated from the expression

$$\frac{T_e}{T_{e0}}=\frac{1}{|\alpha_1|^2\left|1+\beta_3\dfrac{1-\gamma_2\Gamma_a}{\alpha_1\alpha_2\Gamma_a}\right|^2} \tag{16}$$

whose denominator is equivalent to the effect of the circulator.

An example of the effect is shown in Fig. 3. The extent of the effect varies depending on the phase of $\beta_3(1-\gamma_2\Gamma_a)/\alpha_1\alpha_2\Gamma_a$. It becomes a maximum when the phases of $\beta_3(1-\gamma_2\Gamma_a)/\alpha_1\alpha_2\Gamma_a$ and $\gamma_2\Gamma_a$ are 180 degrees and is a minimum when those phases are 0 and 180 degrees, respectively. The average effect can be obtained by assuming a power summation shown as

$$\left|1+\beta_3\frac{1-\gamma_2\Gamma_a}{\alpha_1\alpha_2\Gamma_a}\right|^2=1+|\beta_3|^2\frac{1+|\gamma_2\Gamma_a|^2}{|\alpha_1\alpha_2\Gamma_a|^2}. \tag{17}$$

In (16), the factor $|\alpha_1|^2$ only means T_{e0} is converted into the equivalent value at the input port, and the other factor

$$\left|1+\beta_3\frac{1-\gamma_2\Gamma_a}{\alpha_1\alpha_2\Gamma_a}\right|^2 \tag{18}$$

implies the effect of the isolation coefficient β_3 from port 1 to port 3. Since (18) can be transformed into

$$\left|\frac{\alpha_1\alpha_2\Gamma_a}{1-\gamma_2\Gamma_a}+\beta_3\right|^2\Big/\left|\frac{\alpha_1\alpha_2\Gamma_a}{1-\gamma_2\Gamma_a}\right|^2 \tag{19}$$

which is equal to the actual gain (10) divided by the assumed gain with β_3 being 0, (19) varies around 1 depending on the phase difference between β_3 and the assumed gain. When the leakage from port 1 to port 3 expressed by β_3 is added to the assumed gain, the noise-temperature reduction effect, from (19), becomes more than 1, and vice versa.

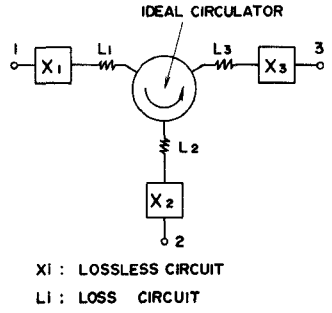

Fig. 4. Equivalent circuit of a circulator.

B. Noise Temperature Increase Caused by the Circulator's Absorption Loss

Since this noise is difficult to analyze using only (3), another equivalent circuit for the circulator shown in Fig. 4 is assumed. This assumption is justified in Appendix III.

Generally, the noise temperature generated by an attenuator whose attenuation is $10\log|L|^2$(dB) is equal to

$$(|L|^2-1)T \tag{20}$$

where T is the physical temperature of the attenuator. Therefore, the noise temperature of L_1 and L_2 of Fig. 4 is equal to

$$(|L_1L_2|^2-1)T_{ac} \tag{21}$$

where T_{ac} is the physical temperature of the circulator. Consequently, by dividing (21) by $|\beta_{121}|^2$ for conversion into the input, the noise temperature caused by the circulator is obtained as follows:

$$T_l=\frac{1}{|\beta_{121}|^2}(|L_1L_2|^2-1)T_{ac} \tag{22}$$

$$\simeq\frac{1}{(1-|\gamma_{111}|^2)}\left\{\frac{(1-|\gamma_{111}|^2)(1-|\gamma_{211}|^2)}{|\alpha_1|^2}-1\right\}T_{ac} \tag{23}$$

$$=\left(\frac{1-|\gamma_{211}|^2}{|\alpha_1|^2}-\frac{1}{1-|\gamma_{111}|^2}\right)T_{ac}. \tag{24}$$

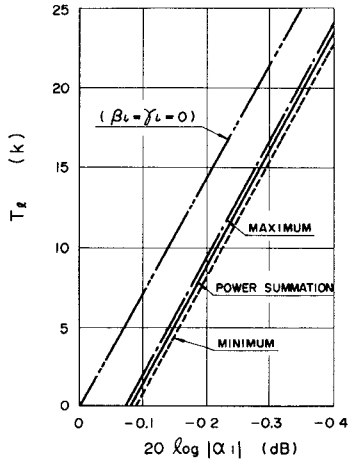

Where $20 \log |\alpha_2| = -0.07$ (dB)

$|\alpha_1| = |\alpha_3|$

$20 \log |\beta_\iota| = \begin{cases} -23\ (\text{dB})\ (\iota = 1,3) \\ -19\ (\text{dB})\ (\iota = 2) \end{cases}$

$20 \log |\gamma_\iota| = \begin{cases} -19\ (\text{dB})\ (\iota = 1) \\ -23\ (\text{dB})\ (\iota = 2) \end{cases}$

$T_{ac} = 298$ (k)

Fig. 5. Relation of T_ℓ versus α_1.

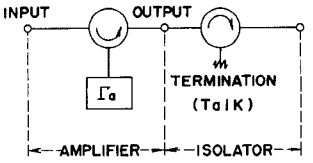

Fig. 6. Amplifier's equivalent circuit including an isolator.

usually, $|\gamma_{111}|^2 \ll 1$ being used as an approximation

$$T_\ell \simeq \left(\frac{1}{|\alpha_1|^2} - 1 - \frac{|\gamma_{211}|^2}{|\alpha_1|^2} - |\gamma_{111}|^2 \right) T_{ac}. \tag{25}$$

Using (A.41) of Appendix III, the noise-temperature increase becomes

$$T_\ell \simeq \left(\frac{1}{|\alpha_1|^2} - 1 - \frac{1}{|\alpha_1|^2} \left| \gamma_2 - \frac{\beta_1 \beta_2}{\alpha_3} \right|^2 - \left| \gamma_1 - \frac{\beta_1 \beta_3}{\alpha_2} \right|^2 \right) T_{ac}. \tag{26}$$

If α_1 is all caused by absorption loss, T_ℓ could be obtained from the first and second terms of (26). In actual fact, however, α_1 partially includes reflection loss and thus requires the third and fourth terms which compensate for the effect of reflection loss at port 2 and 1, respectively. An example of T_ℓ is shown in Fig. 5.

C. Noise Temperature Increase Caused by the Isolator

Usually, an isolator follows a reflection-type amplifier as shown in Fig. 6. The noise corresponding to the physical temperature T_{ai} of the isolator is injected into port 3 and degrades the noise-temperature performance.

Assuming $E_s = 0$, $E_n = 0$, $a_3 \neq 0$, $a_1 = 0$, and $a_2 = \Gamma_a b_2$ in Fig. 1,

$$\frac{b_3}{a_3} = \gamma_3 + \frac{\alpha_2 \beta_2 \Gamma_a}{1 - \gamma_2 \Gamma_a} \tag{27}$$

then the noise-temperature increase becomes

$$T_f = \frac{1}{|\Gamma_0|^2} \left| \gamma_3 + \frac{\alpha_2 \beta_2 \Gamma_a}{1 - \gamma_2 \Gamma_a} \right|^2 T_{ai} \tag{28}$$

$$= \left| \frac{\Gamma_a(\alpha_2 \beta_2 - \gamma_2 \gamma_3) + \gamma_3}{\Gamma_a(\alpha_1 \alpha_2 - \gamma_2 \beta_3) + \beta_3} \right|^2 T_{ai}. \tag{29}$$

Usually, $|\gamma_2 \beta_3| \ll |\alpha_1 \alpha_2|$ and $|\beta_3| \ll |\alpha_1 \alpha_2 \Gamma_a|$; thus, as an approximation

$$T_f \simeq \left| \frac{\beta_2}{\alpha_1} - \frac{\gamma_2 \gamma_3}{\alpha_1 \alpha_2} + \frac{\gamma_3}{\alpha_1 \alpha_2 \Gamma_a} \right|^2 T_{ai}. \tag{30}$$

The first term is the main contribution, governed by the isolation coefficient from port 3 to port 2. The third term is the secondary contribution corresponding to the reflection coefficient of port 3 and the second term has a comparatively low contribution. An example is shown in Fig. 7.

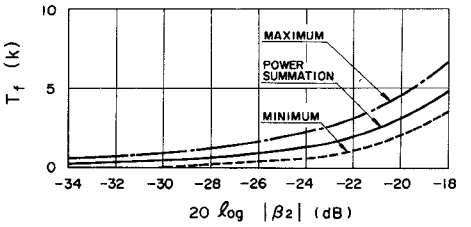

Where $20 \log |\Gamma_a| = 13$ (dB)

$20 \log |\alpha_\iota| = \begin{cases} -0.14\ (\text{dB})\ (\iota = 1) \\ -0.07\ (\text{dB})\ (\iota = 2) \end{cases}$

$20 \log |\gamma_\iota| = -23$ (dB) $(\iota = 2,3)$

$T_{a\iota} = 298$ (k)

Fig. 7. Relation of T_f versus β_2.

D. Overall Degradation

Summing up these three noise-temperature contributions, the noise-temperature degradation of the LNA is given by

$$\Delta T_n = (T_e - T_{e0}) + T_\ell + T_f. \tag{31}$$

This degradation comes closer to 0 as the performance of the circulator becomes more ideal.

IV. Noise Temperature Increase Introduced by the Actual Antenna

The actual antenna can be considered as a combination of an ideal antenna and a lossless circuit as shown in Fig. 8. Including the lossless circuit into the circulator, a new circulator which treats the reference point A as the new port 1 is defined. The new circulator's theoretical expression is shown in Appendix IV.

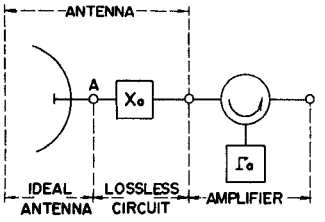

Fig. 8. Equivalent circuit where an antenna is connected to the amplifier.

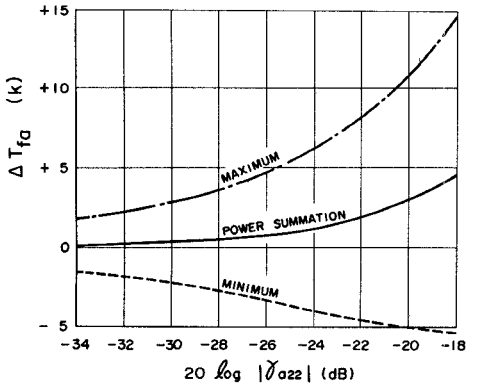

Fig. 9. Noise temperature variation caused by an antenna.

Firstly, T_e' corresponding to T_e becomes

$$T_e' = |\beta_{a21}|^2 \frac{T_{e0}}{|\alpha_1'|^2 \left|1+\beta_3' \dfrac{1-\gamma_2'\Gamma_a}{\alpha_1'\alpha_2'\Gamma_a}\right|^2} \tag{32}$$

by substituting (A.44) through (A.52) into (14) and multiplying $|\beta_{a21}|^2$ for conversion into the original input, the approximation $T_e' \simeq T_e$ is obtained.

Next, T_ℓ' corresponding to T_ℓ becomes

$$T_l' = |\beta_{a21}|^2 \frac{1}{|\beta_{121}'|^2}\left(|L_1L_2|^2-1\right)T_{ac} \tag{33}$$

by substituting (A.53) into (22) and also multiplying $|\beta_{a21}|^2$ as mentioned above. Using (A.57), approximately

$$T_\ell \simeq \frac{1}{|\beta_{121}|^2}\left(|L_1L_2|^2-1\right)T_{ac} \tag{34}$$

consequently, $T_\ell' \simeq T_\ell$ is obtained.

Finally, T_{fa} corresponding to T_f becomes, substituting (A.44) through (A.52) into (30) in a similar manner as above,

$$T_{fa} = |\beta_{a21}|^2 \left|\frac{\beta_2'}{\alpha_1'} - \frac{\gamma_2'\gamma_3'}{\alpha_1'\alpha_2'} + \frac{\gamma_3'}{\alpha_1'\alpha_2'\Gamma_a}\right|^2 T_{ai} \tag{35}$$

and then approximately

$$T_{fa} \simeq \left|\frac{\beta_2}{\alpha_1} + \alpha_3\gamma_{a22} - \frac{\gamma_2\gamma_3}{\alpha_1\alpha_2} + \frac{\gamma_3}{\alpha_1\alpha_2\Gamma_a}\right|^2 T_{ai}. \tag{36}$$

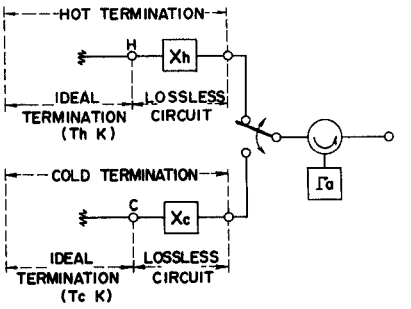

Fig. 10. Measurement circuit of noise temperature.

The noise-temperature degradation caused by the reflection of the antenna is therefore expressed only by the second term of (36). The process of this noise contribution is that the noise from the isolator to port 1 via the attenuation factor of α_3 is reflected by the reflection coefficient of γ_{a22}. The noise expressed as $\alpha_3\gamma_{a22}$ is added to the original noise in the relation of voltage summation, power summation, or voltage cancellation depending on the phase of $\alpha_3\gamma_{a22}$. In the case of power summation, the noise temperature degradation is

$$\Delta T_{fa} \simeq |\alpha_3\gamma_{a22}|^2 T_{ai}. \tag{37}$$

It's maximum and minimum values correspond to

$$\Delta T_{fa} = \left\{|\alpha_2\gamma_{a22}| \pm \left(\left|\frac{\beta_2}{\alpha_1}\right| + \left|\frac{\gamma_2\gamma_3}{\alpha_1\alpha_2}\right| + \left|\frac{\gamma_3}{\alpha_1\alpha_2\Gamma_a}\right|\right)\right\}^2 T_{ai}$$

$$-\left(\left|\frac{\beta_2}{\alpha_1}\right| + \left|\frac{\gamma_2\gamma_3}{\alpha_1\alpha_2}\right| + \left|\frac{\gamma_3}{\alpha_1\alpha_2\Gamma_a}\right|\right)^2 T_{ai} \tag{38}$$

where + and − signs are applied, respectively. An example is shown in Fig. 9.

V. Noise Temperature Measurement Error

The equivalent circuit of the HOT/COLD load measurement is expressed as shown in Fig. 10 applying similar ideas as described in the previous section. Assuming the scattering matrices of the lossless circuits X_h and X_c to be

$$\begin{bmatrix} \gamma_{h11} & \beta_{h12} \\ \beta_{h21} & \gamma_{h22} \end{bmatrix} \quad \begin{bmatrix} \gamma_{c11} & \beta_{c12} \\ \beta_{c31} & \gamma_{c22} \end{bmatrix} \tag{39}$$

respectively, the noise temperature at the reference point H becomes, based on the analogy of (36)

$$\frac{1}{|\beta_{h21}|^2}(T_e + T_\ell + T_{fh}) \tag{40}$$

where

$$T_{fh} \simeq \left|\frac{\beta_2}{\alpha_1} + \alpha_3\gamma_{h22} - \frac{\gamma_2\gamma_3}{\alpha_1\alpha_2} + \frac{\gamma_3}{\alpha_1\alpha_2\Gamma_a}\right|^2 T_{ai}$$

and that at the reference point C,

$$\frac{1}{|\beta_{c21}|^2}(T_e + T_\ell + T_{fc}) \tag{41}$$

where

$$T_{fc} \simeq \left| \frac{\beta_2}{\alpha_1} + \alpha_3 \gamma_{c22} - \frac{\gamma_2 \gamma_3}{\alpha_1 \alpha_2} + \frac{\gamma_3}{\alpha_1 \alpha_2 \Gamma_a} \right|^2 T_{ai}.$$

Assuming the physical temperatures of the HOT/COLD loads to be T_h and T_c (K), respectively, the measured Y factor becomes, by using (40) and (41)

$$Y = \frac{T_h + (T_e + T_\ell + T_{fh})/|\beta_{h21}|^2}{T_c + (T_e + T_\ell + T_{fc})/|\beta_{c21}|^2} \tag{42}$$

usually

$$\left.\begin{aligned} |\beta_{h21}|^2 &= 1 - |\gamma_{h11}|^2 \\ |\beta_{c21}|^2 &= 1 - |\gamma_{c11}|^2 \\ |\gamma_{h11}|^2, |\gamma_{c11}|^2 &\ll 1 \end{aligned}\right\} \tag{43}$$

being considered, (42) is approximately written

$$\gamma = \frac{T_h + (T_e + T_\ell + T_{fh})(1 + |\gamma_{h11}|^2)}{T_c + (T_e + T_\ell + T_{fc})(1 + |\gamma_{c11}|^2)}. \tag{44}$$

Expressing

$$\left.\begin{aligned} T_{fh} &= T_f + \Delta T_{fh} \\ T_{fc} &= T_f + \Delta T_{fc} \end{aligned}\right\} \tag{45}$$

and assuming that the real value of the noise temperature to be measured is

$$T_n = T_e + T_\ell + T_f \tag{46}$$

Y factor becomes

$$Y = \frac{T_h + T_n + \Delta T_{nh}}{T_c + T_n + \Delta T_{nc}} \tag{47}$$

where

$$\Delta T_{nh} = \Delta T_{fh} + |\gamma_{h11}|^2 (T_n + \Delta T_{fh})$$
$$\Delta T_{nc} = \Delta T_{fc} + |\gamma_{c11}|^2 (T_n + \Delta T_{fc}).$$

Consequently, (47) can be transformed into

$$\frac{T_h - YT_c}{Y-1} = T_n + \frac{Y\Delta T_{nc} - \Delta T_{nh}}{Y-1}. \tag{48}$$

Since the left-hand term of (48) is the equation used to calculate the noise temperature using the measured Y factor, it should be equal to T_n in ideal case. However, it differs from T_n by

$$\frac{Y\Delta T_{nc} - \Delta T_{nh}}{Y-1} \tag{49}$$

which corresponds to the measurement error.

Though the reflection coefficient of a usual termination is less than -20 dB, that of HOT load specially designed for measurement purpose can be reduced below -32 dB. A COLD load reflection coefficient of less than -26 dB can be attained, in spite of the disadvantage of having a more complicated configuration which includes a liquid nitrogen coolant. Therefore, considering

$$-10\log|\gamma_{h11}|^2 \geq 32, \quad -10\log|\gamma_{c11}|^2 \geq 26 \tag{50}$$

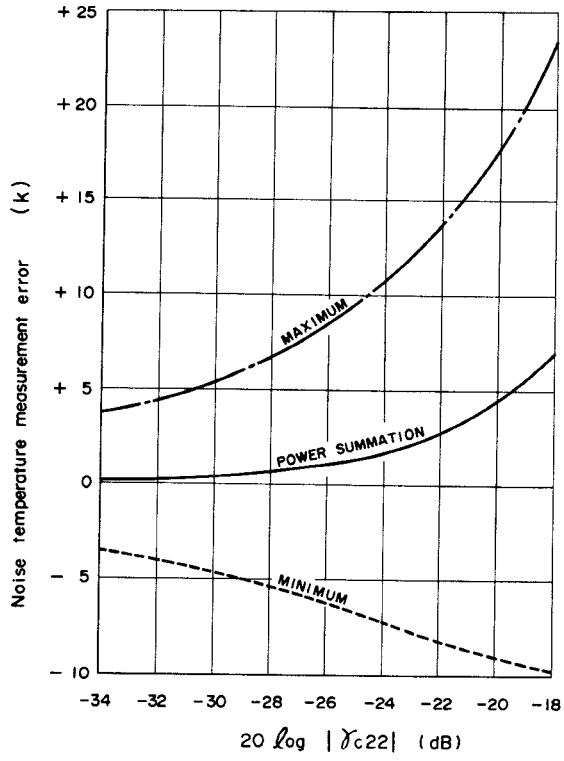

Fig. 11. Measurement error of noise temperature.

the measurement error around $T_n \simeq 40$ K becomes

$$\frac{Y\Delta T_{nc} - \Delta T_{nh}}{Y-1} \simeq \frac{Y\Delta T_{fc} - \Delta T_{fh}}{Y-1}. \tag{51}$$

An example of the error is shown in Fig. 11 when $T_n = 40$ K, $T_h = 298$ K, and $T_c = 80$ K are assumed.

It is found that considerable error could occur as the reflection coefficients of the HOT/COLD load and the circulator becomes larger. Consequently, it is desirable to reduce those coefficients below at least -26 dB and less than -32 dB for the best results.

VI. Conclusion

The noise generated by the parametric amplifier proper is mainly influenced by α_1 and β_3. The noise generated in the circulator itself originates from its actual loss which corresponds to the attenuation from port 1 to port 2 less the reflection loss of ports 1 and 2. The noise contribution introduced by the isolator is mainly governed by β_2.

The noise-temperature degradation, introduced by connection to an actual antenna, roughly corresponds to the partially reflected noise from the isolator by the residual reflection of the antenna. In detail, it varies depending on the phase difference between the reflected noise from the antenna and the original noise, and, in case of voltage summation, reaches a considerably higher value than the value estimated only by the residual reflection of the antenna.

Similarly, the measurement error of the HOT/COLD loads roughly corresponds to the partially reflected noise from the isolator by the residual reflection coefficients of those

loads. Depending on the phase relation between the reflected noise and the original noise, the error varies over a very wide range.

The examples calculated based on the analysis have indicated the rather alarming errors which are mainly caused by the poor 23-dB isolation. Consequently, those alarming errors would be significantly reduced if the circulator's isolation was improved to near 30 dB.

In conclusion, the results of this paper have significantly improved the design capability in assessing the total noise-temperature performance of a satellite communications LNA subsystem.

Appendix I
Scattering Matrix of the Circulator in its Overall Sense

Cascading (2) with (1), (3) is related to (2) and (1) as follows:

$$\gamma_1 = \frac{\gamma_{11} + (\beta_{12}\beta_{21} - \gamma_{11}\gamma_{22})\gamma_{10}}{1 - \gamma_{10}\gamma_{22}} \simeq \gamma_{11} + \beta_{12}\beta_{21}\gamma_{10} \tag{A.1}$$

$$\gamma_2 = \gamma_{20} + \alpha_{10}\frac{\gamma_{22}\beta_{10}}{1 - \gamma_{10}\gamma_{22}} \simeq \gamma_{20} + \alpha_{10}\beta_{10}\gamma_{22} \tag{A.2}$$

$$\gamma_3 = \gamma_{30} + \beta_{30}\frac{\gamma_{22}\alpha_{30}}{1 - \gamma_{10}\gamma_{22}} \simeq \gamma_{30} + \beta_{30}\alpha_{30}\gamma_{22} \tag{A.3}$$

$$\alpha_1 = \frac{\beta_{21}}{1 - \gamma_{10}\gamma_{22}}\alpha_{10} \simeq \beta_{21}\alpha_{10} \tag{A.4}$$

$$\alpha_2 = \alpha_{20} + \beta_{30}\frac{\gamma_{22}\beta_{10}}{1 - \gamma_{10}\gamma_{22}} \simeq \alpha_{20} \tag{A.5}$$

$$\alpha_3 = \frac{\beta_{12}}{1 - \gamma_{10}\gamma_{22}}\alpha_{30} \simeq \beta_{12}\alpha_{30} \tag{A.6}$$

$$\beta_1 = \frac{\beta_{12}}{1 - \gamma_{10}\gamma_{22}}\beta_{10} \simeq \beta_{12}\beta_{10} \tag{A.7}$$

$$\beta_2 = \beta_{20} + \alpha_{10}\frac{\gamma_{22}\alpha_{30}}{1 - \gamma_{10}\gamma_{22}} \simeq \beta_{20} + \alpha_{10}\alpha_{30}\alpha_{22} \tag{A.8}$$

$$\beta_3 = \frac{\beta_{21}}{1 - \gamma_{10}\gamma_{22}}\beta_{30} \simeq \beta_{21}\beta_{30}. \tag{A.9}$$

Approximate equations are obtained by assuming $|\gamma_{11}\gamma_{22}|$, $|\gamma_{10}\gamma_{22}| \ll 1$).

Appendix II
Incident Noise Power at Port 2

From (12), a_2 becomes

$$a_2 = \frac{E_n}{\sqrt{Z_0}\left\{(1+\gamma_2) + \dfrac{1+\Gamma_a}{1-\Gamma_a}(1-\gamma_2)\right\}} \tag{A.10}$$

and thus it is transformed into

$$|a_2|^2 = \frac{|E_n|^2}{Z_0\left|(1+\gamma_2) + \dfrac{1+\Gamma_a}{1-\Gamma_a}(1-\gamma_2)\right|^2} \cdot \frac{Z_g + Z_g^*}{Z_g + Z_g^*}. \tag{A.11}$$

Assuming

$$Z_g = -R + jX \tag{A.12}$$

and using

$$\frac{Z_g}{Z_0} = \frac{1+\Gamma_a}{1-\Gamma_a} \tag{A.13}$$

(A.11) is expressed as

$$|a_2|^2 = \frac{\dfrac{|E_n|^2}{-2R}\left(\dfrac{1+\Gamma_a}{1-\Gamma_a} + \dfrac{1+\Gamma_a^*}{1-\Gamma_a^*}\right)}{\left\{1+\gamma_2 + \dfrac{1+\Gamma_a}{1-\Gamma_a}(1-\gamma_2)\right\}\left\{1+\gamma_2^* + \dfrac{1+\Gamma_a^*}{1-\Gamma_a^*}(1-\gamma_2^*)\right\}}$$

$$= \frac{|E_n|^2}{4R} \cdot \frac{\Gamma_a\Gamma_a^* - 1}{(1-\gamma_2\Gamma_a)(1-\gamma_2^*\Gamma_a^*)}. \tag{A.14}$$

Consequently, it concluded that

$$|a_2|^2 = \{\text{exchangeable noise power [4]}\}\frac{|\Gamma_a|^2 - 1}{|1-\gamma_2\Gamma_a|^2}. \tag{A.15}$$

Appendix III
Scattering Matrix of the Equivalent Circuit Shown in Fig. 4

Firstly, a symmetrical circulator is introduced as the basis for the justification of the equivalent circuit and characterized by the scattering matrix

$$\begin{bmatrix} \gamma_0 & \beta_0 & \alpha_0 \\ \alpha_0 & \gamma_0 & \beta_0 \\ \beta_0 & \alpha_0 & \gamma_0 \end{bmatrix}. \tag{A.16}$$

The eigenvalues of (A.16) becomes [5]

$$\left.\begin{aligned} \lambda_0 &= \alpha_0 + \beta_0 + \gamma_0 \\ \lambda_{+1} &= \alpha_0 e^{j\Psi} + \beta_0 e^{-j\Psi} + \gamma_0 \\ \lambda_{-1} &= \alpha_0 e^{-j\Psi} + \beta_0 e^{j\Psi} + \gamma_0 \end{aligned}\right\} \tag{A.17}$$

where $\Psi = 2\pi/3$. Thus, the eigenvalues of an ideal circulator ($\alpha_0 = 1, \beta_0 = 0, \gamma_0 = 0$) are expressed as

$$\left.\begin{aligned} \lambda_{00} &= 1 \\ \lambda_{+10} &= e^{j\Psi} \\ \lambda_{-10} &= e^{-j\Psi} \end{aligned}\right\}. \tag{A.18}$$

The ideal circulator is characterized by three eigennetworks whose reflection coefficients correspond to (A.18), respectively, as shown in Fig. 12 [6].

Now, assuming that the eigennetworks of the symmetrical circulator is composed of the ideal circulator and the two-port network as shown in Fig. 12, the following rela-

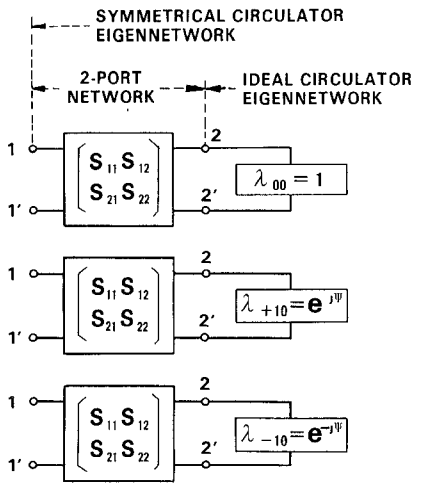

Fig. 12. Eigennetwork of a symmetrical circulator.

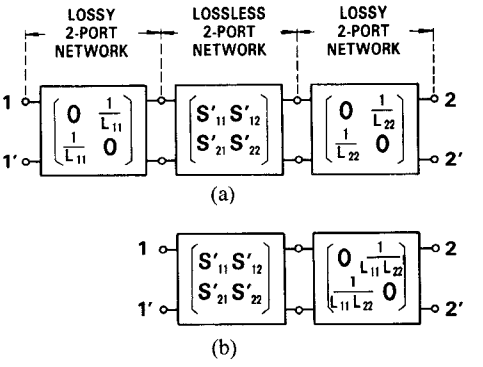

Where $S'_{12}=S'_{21}$

$|S'_{11}|=|S'_{22}|$

$|S'_{11}|^2+|S'_{12}|^2=1$

Fig. 13. Synthesis of a lossy two-port network.

tions can be derived from this combination:

$$\lambda_m=S_{11}+\frac{S_{12}S_{21}}{\frac{1}{\lambda_{m0}}-S_{22}} \tag{A.19}$$

where $m=0,+1,-1$. Assuming that the two-port network is a reciprocal network, it is characterized by

$$S_{12}=S_{21}. \tag{A.20}$$

Consequently, the following relations are derived from (A.19) and (A.17):

$$\left.\begin{aligned} S_{11}&=\gamma_0-\frac{\beta_0^2}{\alpha_0}\\ S_{12}^2&=\alpha_0\left(1-\frac{\gamma_0^3}{\alpha_0^3}\right)\\ S_{22}&=\frac{\beta_0}{\alpha_0}\end{aligned}\right\}. \tag{A.21}$$

Since the symmetrical circulator is lossy, one has

$$1-|\alpha_0|^2-|\beta_0|^2-|\gamma_0|^2>0 \tag{A.22}$$

and thus this is approximately transformed into

$$|\alpha_0|<1-\frac{|\beta_0|^2+|\gamma_0|^2}{2}. \tag{A.23}$$

The ideal circulator defined in [6] is characterized by

$$|\beta_0|=|\gamma_0| \tag{A.24}$$

and moreover, an actual circulator usally expresses the relation

$$|\beta_0|\simeq|\gamma_0|. \tag{A.25}$$

Therefore (A.23) is approximately transformed into

$$|\alpha_0|<1-|\beta_0|^2 \text{ or } 1-|\gamma_0|^2. \tag{A.26}$$

On the other hand, usually

$$\left.\begin{aligned} &|\alpha_0|^2\simeq 1\\ &|\alpha_0|^2\gg|\beta_0|^2,\quad |\gamma_0|^2\end{aligned}\right\} \tag{A.27}$$

being considered, one has

$$\left.\begin{aligned} |S_{12}|^2+|S_{11}|^2&\simeq|\alpha_0|+|\gamma_0|^2\\ |S_{12}|^2+|S_{22}|^2&\simeq|\alpha_0|+\beta_0|^2\end{aligned}\right\}. \tag{A.28}$$

Using (A.26), (A.28) is transformed into

$$\left.\begin{aligned} |S_{12}|^2+|S_{11}|^2&<1\\ |S_{12}|^2+|S_{22}|^2&<1\end{aligned}\right\}. \tag{A.29}$$

Consequently, the two-port network can be composed of a passive network and the symmetrical circulator can be expressed by an ideal circulator whose each port is connected to a reciprocal passive network.

In addition, the two-port network can be expressed as shown in Fig. 13(a). Those parameters defined in Fig. 13(a) are related to the scattering parameters of the two-port network as follows:

$$\left.\begin{aligned} S'_{11}&=S_{11}L_{11}^2\\ S'_{12}&=S_{12}L_{11}L_{22}\\ S'_{22}&=S_{22}L_{22}^2\end{aligned}\right\} \tag{A.30}$$

where

$$\frac{1}{|L_{11}|^4}=|S_{12}|^2\left|\frac{S_{11}}{S_{22}}\right|+|S_{11}|^2$$

$$\frac{1}{|L_{22}|^4}=|S_{12}|^2\left|\frac{S_{22}}{S_{11}}\right|+|S_{22}|^2$$

$$\frac{1}{|L_{11}L_{22}|^2}=|S_{12}|^2+|S_{11}S_{22}|.$$

Usually

$$|L_{11}|\simeq 1 \tag{A.31}$$

being considered, (A.30) is approximately transformed into

$$\left.\begin{aligned} S'_{11}&\simeq S_{11}\\ S'_{12}&=S_{12}L_{11}L_{22}\\ S'_{22}&\simeq S_{22}L_{11}^2L_{22}^2\end{aligned}\right\}. \tag{A.32}$$

Thus, the two-port network can be approximately expressed as shown in Fig. 13(b). Consequently, it is also possible to consider the symmetrical circulator is approximately equivalent to an ideal circulator whose each port is connected to a two-port network as shown in Fig. 13(b).

Finally, the asymmetrical circulator characterized by the scattering matrix (2) can be expressed by the equivalent circuit mentioned above where the parameters shown in Fig. 13(b) is slightly varied port by port, because the scattering parameters of (2) deviate from (A.16) by a small extent.

Similarly, the circulator in its overall sense characterized by the scattering matrix (3) can also be expressed by the same equivalent circuit as above by cascading (1) with the two-port network included in port 1 of the asymmetrical circulator. And thus it is possible to express the circulator in its overall sense as shown in Fig. 4.

In Fig. 4, assuming the scattering matrix of the lossless circuits X_i to be

$$\begin{bmatrix} \gamma_{i11} & \beta_{i12} \\ \beta_{i21} & \gamma_{i22} \end{bmatrix} \tag{A.33}$$

where

$$|\gamma_{i11}| = |\gamma_{i22}| \qquad \beta_{i12} = \beta_{i21} \qquad |\gamma_{i11}|^2 + |\beta_{i12}|^2 = 1$$

that of the loss circuits L_i to be

$$\begin{bmatrix} 0 & 1/L_i \\ 1/L_i & 0 \end{bmatrix} \tag{A.34}$$

and that of the ideal circulator to be

$$\begin{bmatrix} 0 & 0 & e^{j\phi_3} \\ e^{j\phi_1} & 0 & 0 \\ 0 & e^{j\phi_2} & 0 \end{bmatrix} \tag{A.35}$$

the overall scattering matrix components are expressed as

$$D\gamma_i = \gamma_{i11} \prod_{i=1}^{3} \frac{L_i}{\beta_{i12}} + e^{j\phi} \frac{1}{L_i} \left(\beta_{i21} - \frac{\gamma_{i11}\gamma_{i22}}{\beta_{i12}} \right) \cdot \frac{\gamma_{(i+1)22}\gamma_{(i+2)22}}{L_{i+1}L_{i+2}\beta_{(i+1)12}\beta_{(i+2)12}} \tag{A.36}$$

$$D\alpha_i = e^{j\phi} i \left\{ \left(\beta_{i21} - \frac{\gamma_{i11}\gamma_{i22}}{\beta_{i12}} \right) \frac{L_{i+2}}{\beta_{i12}\beta_{(i+2)12}} + \frac{\gamma_{i11}\gamma_{i22}L_{i+2}}{\beta_{i12}^2\beta_{(i+2)12}} \right\} \tag{A.37}$$

$$D\beta_i = e^{j(\phi-\phi_i)} \left\{ \left(\beta_{(i+1)21} - \frac{\gamma_{(i+1)11}\gamma_{(i+1)22}}{\beta_{(i+1)12}} \right) \cdot \frac{\gamma_{(i+2)22}}{L_{i+2}\beta_{(i+1)12}\beta_{(i+2)12}} + \frac{\gamma_{(i+1)11}\gamma_{(i+1)22}\gamma_{(i+2)22}}{L_{i+2}\beta_{(i+1)12}^2\beta_{(i+2)22}^2} \right\} \tag{A.38}$$

where

$$D = \prod_{i=1}^{3} \frac{L_i}{\beta_{i12}} - e^{j\phi} \prod_{i=1}^{3} \frac{\gamma_{i22}}{L_i\beta_{i12}}$$

$$\phi = \sum_{i=1}^{3} \phi i$$

and $i+1$ and $i+2$ corresponding to 4 or 5 reads 1 or 2, respectively. Usually, $|\gamma_{i22}| \ll 1$ being considered, it is possible to assume approximately

$$D \simeq \prod_{i=1}^{3} \frac{L_i}{\beta_{i12}} \tag{A.39}$$

and then the overall scattering matrix components are approximately expressed as

$$\left.\begin{aligned} \gamma_i &\simeq \gamma_{i11} + \frac{\beta_{i21}\beta_{i12}\gamma_{(i+1)22}\gamma_{(i+2)22}}{L_1^2L_2^2L_3^2} \\ \alpha_i &\simeq \frac{\beta_{i21}\beta_{(i+1)12}}{L_iL_{i+1}} \\ \beta_i &\simeq \frac{\beta_{i12}\beta_{(i+1)21}\gamma_{(i+2)22}}{L_1L_2L_3L_{i+2}} \end{aligned}\right\} \tag{A.40}$$

where $e^{j}\phi i/L_iL_{i+1}$ is newly converted into $1/L_iL_{i+1}$. Consequently, the following relation is obtained:

$$\gamma_{i11} = \gamma_i - \frac{\beta_i\beta_{i+2}}{\alpha_{i+1}}. \tag{A.41}$$

Appendix IV
Scattering Matrix of the Circulator Including the Lossless Circuit X_a shown in Fig. 8

Assuming the scattering matrix of the lossless circuit X_a to be

$$\begin{bmatrix} \gamma_{a11} & \beta_{a12} \\ \beta_{a21} & \gamma_{a22} \end{bmatrix} \tag{A.42}$$

where

$$|\gamma_{a11}| = |\gamma_{a22}, \beta_{a12} = \beta_{a21}, |\gamma_{a11}|^2 + |\beta_{a12}|^2 = 1$$

and the scattering matrix of the circulator including X_a to be

$$\begin{bmatrix} \gamma_1' & \beta_1' & \alpha_3' \\ \alpha_1' & \gamma_2' & \beta_2' \\ \beta_3' & \alpha_2' & \gamma_3' \end{bmatrix} \tag{A.43}$$

based on Appendix I, the components of (A.43) are approximately expressed as, because of $|\gamma_{a11}\gamma_{a22}|, |\gamma_1\gamma_{a22}| \ll 1$,

$$\gamma_1' \simeq \gamma_{a11} + \beta_{a12}^2\gamma_1 \tag{A.44}$$

$$\gamma_2' \simeq \gamma_2 + \alpha_1\beta_1\gamma_{a22} \tag{A.45}$$

$$\gamma_3' \simeq \gamma_3 + \beta_3\alpha_3\gamma_{a22} \tag{A.46}$$

$$\alpha_1' \simeq \beta_{a21}\alpha_1 \tag{A.47}$$

$$\alpha_2' \simeq \alpha_2 \tag{A.48}$$

and

$$\alpha_3' \simeq \beta_{a12}\alpha_3 \tag{A.49}$$

$$\beta_1' \simeq \beta_{a12}\beta_1 \tag{A.50}$$

$$\beta_2' \simeq \beta_2 + \alpha_1\alpha_3\gamma_{a22} \tag{A.51}$$

$$\beta_3' \simeq \beta_{a21}\beta_3. \tag{A.52}$$

When X_a is connected to the circulator characterized by Fig. 4, the overall scattering matrix components can be obtained by applying the scattering matrix of the combined lossless circuit X_1' of X_a and X_1 as follows:

$$\begin{bmatrix} \gamma_{111}' & \beta_{112}' \\ \beta_{121}' & \gamma_{122}' \end{bmatrix} \tag{A.53}$$

where

$$\gamma_{111}' = \gamma_{a11} + \frac{\beta_{a12}\beta_{a21}\gamma_{111}}{1-\gamma_{a22}\gamma_{111}} \simeq \gamma_{a11} + \beta_{a12}\beta_{a21}\gamma_{111} \tag{A.54}$$

$$\gamma_{122}' = \gamma_{122} + \frac{\beta_{112}\beta_{121}\gamma_{a22}}{1-\gamma_{a22}\gamma_{111}} \simeq \gamma_{122} + \beta_{112}\beta_{121}\gamma_{a22} \tag{A.55}$$

$$\beta_{112}' = \frac{\beta_{a12}\beta_{112}}{1-\gamma_{a22}\gamma_{111}} \simeq \beta_{a12}\beta_{112} \tag{A.56}$$

$$\beta_{121}' = \frac{\beta_{a21}\beta_{121}}{1-\gamma_{a22}\gamma_{111}} \simeq \beta_{a21}\beta_{121}. \tag{A.57}$$

Approximate equations are obtained by assuming $|\gamma_{a22}\gamma_{111}| \ll 1$.

Acknowledgment

The author wishes to thank Dr. T. Kawahashi, Dr. Y. Kaito, R. Tamura, S. Yokoyama, and the staff of Nippon Electric Co., Ltd., who participated in this study, for their encouragements and cooperation.

References

[1] R. C. Knechtli and R. D. Weglein, "Low noise parametric amplifier," *Proc. IRE*, vol. 48, pp. 1218–1226, July 1960.

[2] J. C. Greene and E. W. Sard, "Optimum noise and gain-bandwidth performance for a practical one-port parametric amplifier," *Proc. IRE*, vol. 48, pp. 1583–1590, Sept. 1960.

[3] T. Mukaihata, B. L. Walsh, M. F. Bottjer, and E. B. Roberts, "Subtle differences in system noise measurements and calibration of noise standards," *IRE Trans. Microwave Theory Tech.*, vol. MTT-10, pp. 506–516, Nov. 1962.

[4] K. Kurokawa, "Power waves and the scattering matrix," *IEEE Trans. Microwave Theory Tech.*, vol. MTT-13, pp. 194–202, Mar. 1965.

[5] H. Bosma, "Performance of loss *H*-plane *Y* circulator," *IEEE Trans. Magn.* (1966 INTERMAG Issue), vol. MAG-2, pp. 273–277, Sept. 1966.

[6] J. Helszajn, "Dissipation and scattering matrices of lossy junctions," *IEEE Trans. Microwave Theory Tech.*, vol. MTT-20, pp. 779–782, Nov. 1972.

Mitsugi Kajikawa was born in Japan, on April 2, 1937. He received the B. E. degree from Tokyo University in 1961.

He joined Nippon Electric Co., Ltd., in 1961 and is now a Manager of Device Development Department, Microwave and Satellite Communications Division. He has been engaged in research and development of low-noise amplifiers for satellite communications.

Mr. Kajikawa is a member of the Institute of Electronics and Communication Engineers of Japan.